NANOMATERIALS SCIENCE & ENGINEERING
Vol. 7, No. 1, pp. 5-13 (2025)

RESEARCH ARTICLE

https://doi.org/10.34624/nmse.v7i1.37480

An innovative approach to wound dressings: citric acid cross-linked carboxymethylcellulose-poly(vinyl alcohol) hydrogels with variable pore sizes

Yağmur CAMCI[1,2,*], Serbülent TÜRK[2,3], Mahmut ÖZACAR[2,4]

[1]Sakarya University, Biomedical Engineering, Institute of Natural Sciences, Esentepe Campus, 54187, Sakarya, Turkey
[2]Biomaterials, Energy, Photocatalysis, Enzyme Technology, Nano & Advanced Materials, Additive Manufacturing, Environmental Applications and Sustainably Research & Development Group (BIOENAMS) R&D Group), 54187, Sakarya, Turkey
[3]BIMAS-RC, (Biomedical, Magnetic and Semiconductor Materials Application and Research Center), Sakarya University, 54187, Sakarya, Turkey
[4]Sakarya University, Science & Arts Faculty, Department of Chemistry, 54187, Sakarya, Turkey
**Corresponding author, e-mail address: yagmur.camci@ogr.sakarya.edu.tr*

Received 14 August 2024; accepted 15 January 2025; published online 31 January 2025

ABSTRACT

Polyvinyl alcohol (PVA)/carboxymethyl cellulose (CMC) hydrogels were fabricated with varying concentrations of CMC. The hydrogels underwent cross-linking using non-toxic and biocompatible citric acid (CA) in combination with the freeze-thaw technique. FTIR analysis confirmed the hydrogels' chemical structures, while SEM characterization determined their pore diameters and porosity ratios. Hydrogels with diverse porosities exhibited suitable pore diameters for skin cells. Moreover, the hydrogels demonstrated a high swelling capacity, and the augmentation of CMC content resulted in increased water retention capacity. Their water vapor transmission, combined with their swelling properties, highlights their potential as suitable materials for use in wound dressings. These biopolymer-based hydrogels show promise for various applications, including wound dressings and biomimetic artificial skin, effectively replicating the properties of the epidermis and dermis.

1. INTRODUCTION

Skin constitutes ~20% of the body weight and is one of our largest organs [1]. Skin from the lower layer to the upper layers (from inside to outside) are listed as hypodermis (subcutaneous tissue), reticular dermis, papillary dermis, stratum basale, stratum spinosum, stratum granulosum, stratum lucidum, and stratum corneum. The predominant cell type of the epidermis is keratinocytes, which are also involved in forming the epidermal water barrier. Moreover, melanocytes manufacture the melanin pigment. Langerhans cells process antigens that enter the skin, and Merkel cells are concentrated in areas where sensory perception occurs immediately, such as the fingertips. In addition, the skin includes hair follicles and skin supplements like hair, sebaceous glands, and sweat glands [2].

The skin, which covers our body from the outside and protects us against physical damage from the environment, is injured throughout life for various reasons, such as injuries, surgery, and burns. These acute wounds heal in an acceptable

This work is licensed under a Creative Commons Attribution-NonCommercial 4.0 International License.

period, and chronic wounds where healing takes longer and complete healing cannot occur.

Physiology of healing of skin injuries covers the stages of hemostasis, inflammation, proliferation, and remodeling [3]. Hemostasis is the body's first response to a wound to reduce blood loss by contracting blood vessels. During the inflammation stage, neutrophils migrate to the injured area and protect the wound against outside microorganisms. The proliferation stage includes granulation tissue beginning to form from the wound base and re-epithelialization [4]. During the remodeling stage, type 1 collagen is replaced by type 3 collagen, and the extracellular matrix is remodeled into a more mature structure with greater integrity [3]. These stages do not occur sequentially but rather in interlocking periods. In addition to traditional wound dressings used in wound healing, alginate dressings, polyurethane foam dressings, hydrogel dressings, hydrocolloid dressings, and nanofiber dressings are being developed to make wound healing more comfortable, support cell regeneration, and protect the wound against pathogens. Apart from wound dressings, artificial skin substitutes have also attracted attention in recent years. If we review these, Epidex, a permanent epidermal skin substitute, was commercially available in Switzerland in 2004 and produced for treating chronic wounds. *MySkin* was named biomedical product of the year in 2008 and is a permanent epidermal skin substitute used to treat chronic ulcers. *Suprathel* is a cell-free temporary epidermal skin substitute used in second and third-degree burn treatments. *Alloderm*, the most widely used brand of acellular dermal matrix, is a permanent dermal substitute. *Dermagraft* is a permanent dermal skin substitute derived from cryopreserved human fibroblast. *Biobrane* is a cell-free dermal skin substitute composed of nylon mesh and a thin layer of silicone, and more commercial products are available in addition to the products mentioned above.

Skin substitutes can be developed under in vitro, in vivo, and ex vivo conditions [5]. The most remarkable skin substitute production methods are the biopsy tissue method and the bioprinting method. In addition to the advantages of these methods, they also have disadvantages, such as ethical problems and difficulties in maintaining cell viability. Therefore, in this study, we focus on hydrogels that offer similar properties to skin. In the realm of literature, "hydrogel skin" encompasses hydrogels that exhibit both flexibility and electrical conductivity [6], [7], [8], in addition to those capable of facilitating drug release [9], [10] and possessing tissue adhesive [11], [12] properties intended for use on the skin.

In the study, we discussed poly(vinyl alcohol) (PVA) and carboxymethyl cellulose (CMC) based hydrogels, which are remarkable in many sectors such as biomedical, food packaging, and agricultural applications. CMC, a derivative of cellulose obtained from natural sources, is a biocompatible, water-soluble, non-toxic, and biodegradable biopolymer. The low strength problem of CMC can be overcome by using it together with PVA [13]. Citric acid (CA) is the cross-linking agent for PVA/CMC-based hydrogels. Classified as "generally recognized as safe" by the Food and Drug Administration [14], citric acid is an aliphatic organic acid known for its environmentally friendly, biodegradable properties. It can be quickly metabolized and eliminated from the body. Citric acid can create both physical and chemical cross-links. It forms cross-links with polymer chains via ionic interactions or hydrogen bonds at room temperature [15] esterifies the hydroxyl groups in nearby polymer chains to create cross-links at high temperatures [16].

2. MATERIALS AND METHODS

2.1. Materials

Polyvinyl alcohol (PVA, Mw: 60000) and citric acid monohydrate (CA, Mw: 210.14) were purchased from Merck, Germany. Carboxymethylcellulose sodium salt (CMC, Melting Point: >300 °C) was purchased from ThermoFisher, Germany. The entire chemicals were of analytical grade and were used as received without any purification.

2.2. Hydrogel Production for Lower Layer

10%wt. PVA solution and 1.66% wt. CMC solution was dissolved in distilled water in separate beakers in a magnetic stirrer. When the PVA solution became clear, the CMC solution was leisurely supplemented while continuing to stir. After mixing

the mixture for a while, CA, 20% of the total polymer weight, was supplemented to the solution. The prepared hydrogel mixture was poured into Petri dishes and under room conditions for 1 night to remove air bubbles. Petri dishes containing a homogeneous hydrogel solution, free of air bubbles, were placed at -20 C for freezing. And 2 cycles of freeze-thaw were applied to the hydrogel (S1). The thawing process was carried out under room conditions.

Similarly, the weight ratio of the hydrogel, S2 polymers, which was later selected as the dermal skin substitute, was PVA: CMC 4:3. In the same way, CA was added 20% by weight of the total polymer, and the Petri dishes were under the room conditions for 1 night to remove air bubbles. After 2 cycles of freeze-thaw, the preparation of hydrogels was completed.

2.3. Hydrogel Production for the Upper Layer

Similar production steps were applied to the hydrogels prepared as dermal layer substitutes and to the hydrogels developed for the epidermal layer substitute. The aim of increasing the CMC and, therefore, the CA ratio in the hydrogel content is to aim for a smaller pore diameter and more cross-linking than the dermal substitute. This hydrogel (S3) was chosen as the epidermal skin substitute and had a PVA: CMC 1:1 weight ratio.

2.4. Characterization of PVA/CMC-Based Hydrogel

Fourier Transform Infrared (FTIR) spectra of lyophilized S1, S2, and S3 hydrogels and PVA, CMC, and CA dry powders were recorded with Spectrum Two FT-IR Spectrometer (PerkinElmer, USA). The samples were scanned in the wavenumber range of 400-4000cm^{-1} (20 scans with a resolution of 4 cm^{-1}).

2.5. Determination of Pore Size

All hydrogels were lyophilized and then cut, and the inner sides cut images of the hydrogels were perused under a field emission scanning electron microscope (FESEM, Quanta 450 FEG). 100x and 500x zoom FESEM images were examined with ImageJ software.

2.6. Swelling Study

The hydrogels were lyophilized and placed in 15 mL volume Falcon centrifuge tubes at room temperature, and the Falcon centrifuge tubes were filled with 10 mL distilled water. The initial weights (W_0) of the hydrogels were determined, and the weights of the hydrogels continued to be measured at regular intervals. The hydrogels' swelling ratios (%) in distilled water can be determined using the following equation:

$$SR\% = ((W_T\text{-}W_0)/W_0) \times 100\% \quad (1)$$

W_0 is the initial weight of the hydrogels, while W_T is the weight of the hydrogels exposed to the application during time (t).

2.7. Water Retention Capacity of Hydrogels

Lyophilized hydrogels were swollen for 24 hours in Falcon centrifuge tubes filled with distilled water. The excess water (bulk water) on the surface of the hydrogel was eliminated with filter paper, and then the weight (W_W) of the hydrogel was determined. Hydrogels were placed in a hot air oven (37 °C) in open-top petri dishes. Water retention capacity (%) was calculated via Eq. (2):

$$WRC\% = ((W_W\text{-}W_D)/W_W) \times 100\% \quad (2)$$

W_W is the initial swollen (wet) weight of the hydrogels. W_D is the weight of hydrogels that lose water (dry) over time.

2.8. Determined of Water Vapor Transmission

Water vapor transmission of hydrogels (WVTH) characterization was performed under room conditions in a desiccator assembly. An open-mouth rectangular container (10.5 cm x 17 cm) was filled with 500 mL of water. The container filled with water was placed in the lower compartment of the desiccator. On top of the desiccator disc was a 50 mL falcon tube (ISOLAB, Turkey) filled with anhydrous calcium chloride. $CaCl_2$ was dried in the oven and weighed before being filled into the tube. The cap part of the $CaCl_2$-filled falcon tube was covered with hydrogel. There is no hygroscopic

material other than $CaCl_2$ in the WVTH assembly. Finally, the $CaCl_2$ kept in the WVTH assembly for 1 night was weighed.

2.9. Gel Fraction Test

The lyophilized hydrogels were cut into square shapes (0.8 mm × 0.8 mm) and weighed 15±0.3 mg (W_0). For one day, hydrogels were swollen in 15 mL falcon tubes as in the swelling test. The excess water was removed from the surface of the hydrogel using filter paper and dried in an oven at 37±1°C for approximately 1 day until the weights of the hydrogels reached equilibrium and their weights were weighed (W_d).

The gel fraction (%) of hydrogels is determined using the following equation:

$$GF\ (\%) = ((W_0 - W_d)/W_0) \times 100\% \quad (3)$$

W_0 is the initial weight of the hydrogels, while W_d is the reached equilibrium weight of the hydrogels.

3. RESULTS AND DISCUSSION

3.1. FTIR Analysis

A broad band of O-H stretching occurs at around 3400 cm^{-1}. The peak at 1086 cm^{-1} is characteristic for the C-O group of PVA [17]. The peak at 1586 cm^{-1} corresponds to the C=O stretching of the CMC carboxylate group. The band between wavelengths 1428 – 1282 cm^{-1} correlates with the CH groups' planar deformation. The band around 1057 cm^{-1} represents the C-O stretching of cellulose, hemicellulose, and aliphatic primary and

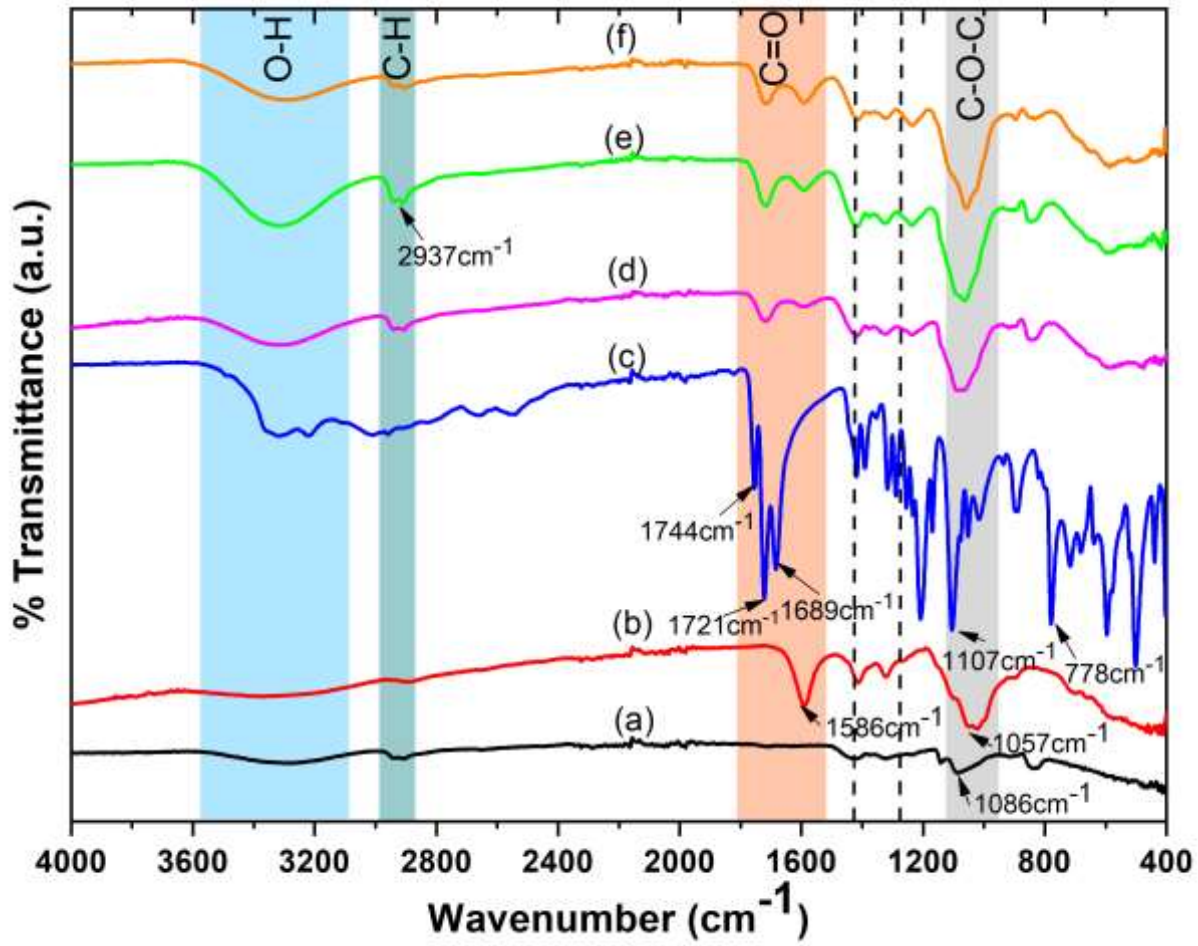

Figure 1. FT-IR spectra of (a) PVA powder, (b) CMC powder, (c) CA powder, (d) S1 hydrogel, (E) S2 hydrogel, (f) S3 hydrogel.

secondary alcohols. The peaks at 1744 cm^{-1}, 1721 cm^{-1}, and 1689 cm^{-1} refer to carboxylic acid and ester bonds [18]. Additionally, the peaks at 1107 cm^{-1} and 778 cm^{-1} are characteristic peaks of CA for C-O and C-C stretchings, respectively. The presence of a peak at 2937 cm^{-1}, corresponding to the saturated aliphatic C-H group in the cellulose chain, and the extension of the C-O-C band of the hydrogels to the 1078 cm^{-1} peak provides further evidence that CA participates in the structure as a cross-linker in the hydrogel matrix.

3.2. Study on the Pore Size of Hydrogels

Human skin cells have an average diameter of 40 μm [19]. The optimal pore size required for skin cell regeneration in adult mammals is 20-125 μm [20]. The predominant cell type of the epidermis is keratinocytes [21]. If the keratinocytes are less than 11 μm in diameter, it is able to proliferate (this can be up to 20 μm), but if the keratinocytes are larger than 20 μm in diameter, they cannot proliferate

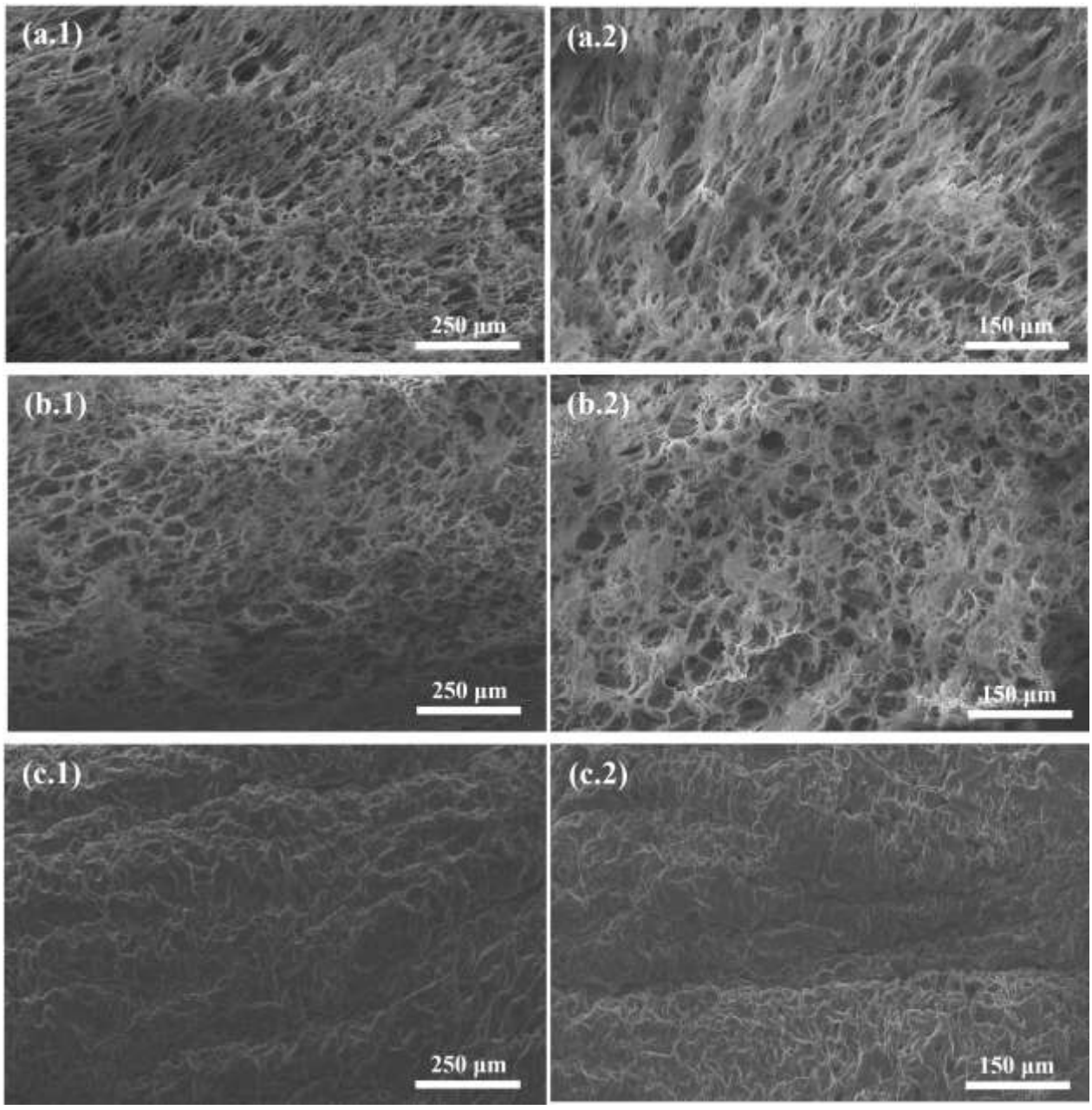

Figure 2. SEM images of hydrogels captured at various magnification levels are represented as follows: (a) S1, (b) S2, and (c) S3.

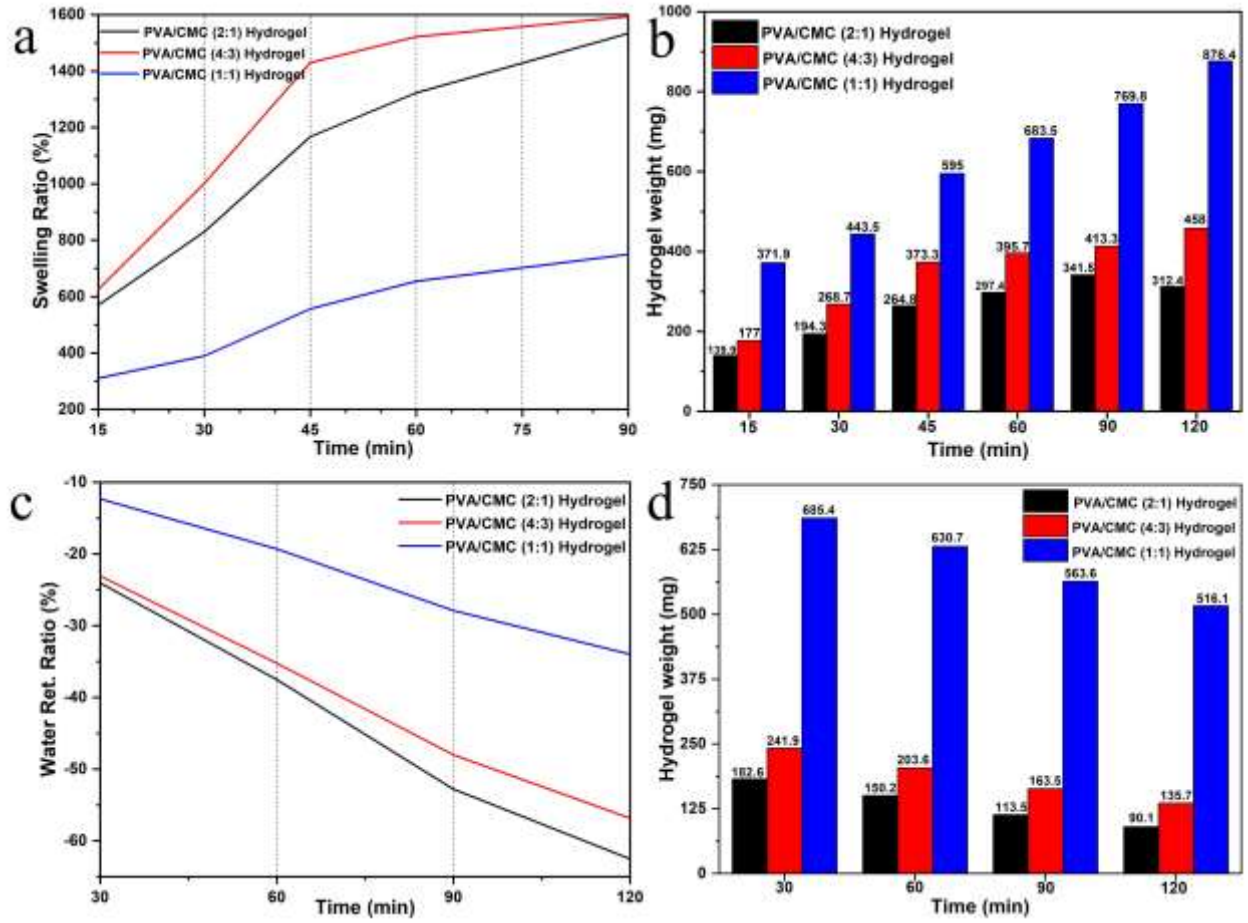

Figure 3. a) Swelling ratio (%) graph, b) Changes in the weight of hydrogels as they swell over time, c) Water retention capacity (%) graph, d) Water loss of hydrogels over time graph.

[22], they grow. Nonproliferating keratinocytes can grow up to 30 μm in diameter [23]. The papillary layer, located just below the epidermis, is rich in collagen (mainly type 1 collagen) and elastic fibrils [21]. Mizukoshi et al., as a result of their studies [24], [25], assumed that the dermal papillary structure' diameter was approximately 20 μm.

S1 has a porosity of 45.479% and pore sizes ranging from 2.714 to 69.158 μm. S2, chosen as the dermal layer substitute, has 63.722% porosity and pore sizes ranging from 2.244 to 73.539 μm. S3, selected as the epidermal skin substitute, has a porosity of 42.529% and pore sizes ranging from 3.429-32.620 μm. Hydrogel artificial skin substitutes with micropore sizes have a pore size appropriate for the regeneration of dermis and epidermis cells and a pore size sufficient for the growth of cells, as supported by the literature. While pores with an average diameter of 40 μm support new cell formation, pores <40 μm serve as cell scaffolds. Moreover, hydrogel artificial skin substitutes are in a range that will not prevent the adhesion of cells (cells cannot attach to >150μm pores [26], [27]). These results, obtained with FE-SEM images and ImageJ software, state that, as intended, the layers have different surface porosity ratios.

3.3. Swelling Analysis

When a dry hydrogel begins to swell in an aqueous environment, the most polar hydrophilic groups begin to hydrate first, called primary-bound water. As the polar groups hydrate and swell, the hydrophobic groups that interact with the remaining water molecules bind to the water, called secondary-bound water [28]. In the study, we noted that with the initial swelling of the hydrogels, their dry weight increased by 5.7 (S1), 6.25 (S2) and 3.1 (S3) times, respectively. The water capacity of the

hydrogels reached equilibrium in approximately 90 minutes. The swelling analysis was continued throughout this period.

The results show that the swelling capacity of the hydrogel changes with the amount of CMC and the cross-linker effect, as reported by Bucak et al. (2022) [29]. Depending on the amount of CMC and total polymer in the hydrogels, the swelling capacity first increased with the increase in the amount of CA. Then, as our predictions and FESEM images show, the amount of water taken into the hydrogel matrix is restricted due to a tight network structure of S3.

3.4. Water Retention Analysis

The hydrogels were swollen for 24 h, and bulk water was removed from the hydrogels with filter paper. The water retention capacities of the hydrogels kept at 37 °C, representing the human body temperature, were determined with Equation 2. The hydrogels, which were measured 4 times, showed weight loss of 24.04%, 23.08%, and 12.31% of their W_W, respectively, in the first half hour. Conclusions show that S1 and S2 exhibited similar water retention capacity results, just like in the swelling analysis. Moreover, after two hours, the hydrogels lost 62.52%, 56.85%, and 34% of their weight. As supported by the literature [29], [30], we can also say that the hydrogel containing more CMC has a higher water retention capacity.
As explained in the introduction, keratinocytes are the dominant cells of the epidermis, and they participate in the epidermal water barrier. S3 provided the closest properties to the epidermal water barrier, having a higher water retention capacity and lower swelling capacity than other hydrogels. Another reason why we chose S3 as an epidermal skin substitute is its pore size (Fig. 2.). Although the hydrogels in our study do not fully provide the epidermal water barrier feature, increasing the amount of CMC shows that it will be effective in making the hydrogels similar to the epidermis layer.

3.5. Water Vapor Transmission

The air permeability of the hydrogel dressing was assessed by examining the water vapor permeability of S2, characterized by the highest pore volume and identified as the dermis equivalent with the highest gel fraction value. PVA/CMC-based hydrogels are designed as biomimic skin equivalents and wound dressings. Wound dressings should not completely deprive the wound of oxygen. They should allow gas inflow and outflow [31]. However, sudden discharge of water vapor dehydrates the wound and may cause the dressing to stick to the wound and cause secondary trauma.

The WVTH test was carried out using a desiccator setup. The water in the lower section of the desiccator evaporated and was retained by the hygroscopic $CaCl_2$ passing through the hydrogel membrane. The desiccator was sealed for one night, and the $CaCl_2$, initially with an oven-dried weight of 49.38 g, increased by 3.36% to reach 51.04 g.

The test, conducted under normal room conditions using a desiccator setup, confirmed that the hydrogel dressing allowed gas to enter the injured area.

3.5. Gelation Degrees of Hydrogels

Gel fraction analysis was performed to obtain information about the cross-linking capacity of hydrogel matrices. Gelling agents are divided into natural and synthetic group ensuring that the material becomes viscous or, in other words, thixotropic [32]. To determine the gelation degrees of PVA/CMC-based hydrogels, the lyophilized hydrogels were swollen and their weights were measured. Then, the hydrogels were dried until they reached their equilibrium weight, and their weights were measured again.

Cellulose derivatives are used as gelling agents. However, as mentioned in the literature [33], CMC-based hydrogels offer a gelation degree of approximately 40%. Similar to the literature, as a result of gel fraction analysis, the gelation degree of S1 (2:1) was measured as 38.73%, the gelation degree of S2 (4:3) as 48.61%, and the gelation degree of S3 (1:1) as 45.33%.

Compared to CMC-based hydrogels, recent hydrogel studies [34], [35] offer gelation degrees of >90%. In this context, the cross-linker ratio (CA ratio) is planned to increase the gelation degrees of CMC-based hydrogels in future studies.

4. CONCLUSIONS

PVA/CMC hydrogels were prepared at different ratios: S1 (2:1), S2 (4:3), and S3 (1:1). A non-toxic cross-linker, CA, was added at 20% by weight of the polymer, and the hydrogels were successfully produced using 2 cycles of the freeze-thaw process. The hydrogels exhibit a notable swelling capacity, which can swell up to 15 times their dry weight. An increased CMC ratio correlates with a higher water retention capacity in the swollen hydrogels. FESEM images analyzed with the ImageJ program show that the pore size of S1 ranges from 2.714 to 69.158 µm. S2 has a pore size ranging from 2.244 to 73.539 µm, and S3 exhibits pore sizes ranging from 3.429 to 32.620 µm. The hydrogels possess diverse pore sizes with suitable pore diameters that facilitate the proliferation and growth of skin cells while also functioning as a scaffold for skin cell growth. In addition to meeting the properties of biomimicry artificial skin, these hydrogels are also suitable for wound dressings; hydrogels have been proven to allow the exchange of gases. The results of the gel fraction of the hydrogels were found to be 43.67±4.94%. CMC-based hydrogels will be supported with different cross-linking techniques in future studies.

ACKNOWLEDGEMENTS

This work was supported by the Scientific Research Projects Commission of Sakarya University (Project Number: 2024-26-62-31).

REFERENCES

[1] M. Halem and C. Karimkhani, “Dermatology of the Head and Neck: Skin Cancer and Benign Skin Lesions,” *Dent Clin North Am*, vol. **56**, no. 4, pp. 771–790, Oct. 2012.

[2] D. H. Chu and C. A. Loomis, “Structure and Development of the Skin and Cutaneous Appendages,” *Fetal and Neonatal Physiology, 2-Volume Set*, pp. 490-498.e1, Jan. 2017.

[3] S. Singh, A. Young, and C. E. McNaught, “The physiology of wound healing,” *Surgery (Oxford)*, vol. **35**, no. 9, pp. 473–477, Sep. 2017.

[4] M. Alhajj, P. Bansal, and A. Goyal, “Physiology, Granulation Tissue,” *StatPearls*, Mar. 2020, Accessed: Dec. **21**, 2023.

[5] E. Sutterby, P. Thurgood, S. Baratchi, K. Khoshmanesh, and E. Pirogova, “Microfluidic Skin-on-a-Chip Models: Toward Biomimetic Artificial Skin,” *Small*, vol. **16**, no. 39, p. 2002515, Oct. 2020.

[6] R. Fu *et al.*, “A Tough and Self-Powered Hydrogel for Artificial Skin,” *Chemistry of Materials*, vol. **31**, no. 23, pp. 9850–9860, Dec. 2019.

[7] S. H. Kim *et al.*, “Ultrastretchable Conductor Fabricated on Skin-Like Hydrogel–Elastomer Hybrid Substrates for Skin Electronics,” *Advanced Materials*, vol. **30**, no. 26, p. 1800109, Jun. 2018.

[8] H. Yuk, T. Zhang, G. A. Parada, X. Liu, and X. Zhao, “Skin-inspired hydrogel–elastomer hybrids with robust interfaces and functional microstructures,” *Nature Communications 2016 7:1*, vol. **7**, no. 1, pp. 1–11, Jun. 2016.

[9] Y. Cai, L. Xin, H. Li, P. Sun, C. Liu, and L. Fang, “Mussel-inspired controllable drug release hydrogel for transdermal drug delivery: Hydrogen bond and ion-dipole interactions,” *Journal of Controlled Release*, vol. **365**, pp. 161–175, Jan. 2024.

[10] P. Dai *et al.*, “A Novel Methacryloyl Chitosan Hydrogel Microneedles Patch with Sustainable Drug Release Property for Effective Treatment of Psoriasis,” *Macromol Biosci*, vol. **23**, no. 12, p. 2300194, Dec. 2023.

[11] H. Jung *et al.*, “Adhesive Hydrogel Patch with Enhanced Strength and Adhesiveness to Skin for Transdermal Drug Delivery,” *Adv Funct Mater*, vol. **30**, no. 42, p. 2004407, Oct. 2020.

. Zeng, “Highly Adhesive Antibacterial Bioactive Composite Hydrogels With Controllable Flexibility and Swelling as Wound Dressing for Full-Thickness Skin Healing,” *Front Bioeng Biotechnol*, vol. **9**, p. 785302, Dec. 2021.

[13] V. Tyagi and A. Thakur, “Carboxymethyl cellulose-polyvinyl alcohol based materials: A review,” *Mater Today Proc*, Jan. 2023.

[14] R. Salihu *et al.*, “Citric acid: A green cross-linker of biomaterials for biomedical applications,” *Eur Polym J*, vol. **146**, Mar. 2021.

[15] P. Kaur *et al.*, “Waste to high-value products: The performance and potential of carboxymethylcellulose hydrogels via the circular economy,” *Cellulose*, vol. 30, no. 5, pp. 2713–2730, Mar. 2023.

[16] W. Zhang, S. Roy, E. Assadpour, X. Cong, and S. M. Jafari, “Cross-linked biopolymeric films by citric acid for food packaging and preservation,” *Adv Colloid Interface Sci*, vol. **314**, Apr. 2023.

[17] V. S. Ghorpade, R. J. Dias, K. K. Mali, and S. I. Mulla, “Citric acid crosslinked carboxymethylcellulose-polyvinyl alcohol hydrogel films for extended release of water soluble basic drugs,” *J Drug Deliv Sci Technol*, vol. **52**, pp. 421–430, Aug. 2019.

[18] F. Siregar, D. Nasution, Y. Muis, D.Y. Kaban, Preparation and characterization of antibacterial film based on carboxymethylcellulose from gebang leaf (Coryphautan), polyvinyl alcohol and citric acid, *Journal of Chemistry* **12** (2019) 554–564.

[19] M. M. Ismail, M. N. Shah Zainudin, R. A. Rahim, M. Alice, and N. Mohd Kassim, “An investigation of electromagnetic field effect on a human skin cell using numerical method approaches,” *IEEE International RF and Microwave Conference, RFM 2011 - Proceedings*, pp. 178–182, 2011.

[20] Z. Zhang, Y. Feng, L. Wang, D. Liu, C. Qin, and Y. Shi, “A review of preparation methods of porous skin tissue engineering scaffolds,” *Mater Today Commun*, vol. **32**, p. 104109, Aug. 2022.

[21] M. H. Ross, and W. Pawlina, Histology, p. 493-500, Lippincott Williams & Wilkins (2006).
[22] Y. Barrandon and H. Green, "Cell size as a determinant of the clone-forming ability of human keratinocytes.," *Proceedings of the National Academy of Sciences*, vol. **82**, no. 16, pp. 5390–5394, Aug. 1985.
[23] T. T. Sun and H. Green, "Differentiation of the epidermal keratinocyte in cell culture: Formation of the cornified envelope," *Cell*, vol. **9**, no. 4 PART 1, pp. 511–521, Dec. 1976.
[24] K. Mizukoshi, K. Yonekura, M. Futagawa, T. Nakamura, K. Hirayama, and K. Takahashi, "Changes in dermal papilla structures due to aging in the facial cheek region," *Skin Research and Technology*, vol. **21**, no. 2, pp. 224–231, May 2015.
[25] K. Mizukoshi, T. Nakamura, and A. Oba, "The relationship between dermal papillary structure and skin surface properties, color, and elasticity," *Skin Research and Technology*, vol. **22**, no. 3, pp. 295–304, Aug. 2016.
[26] B. K. H. L. Boekema *et al.*, "Effect of pore size and cross-linking of a novel collagen-elastin dermal substitute on wound healing," *J Mater Sci Mater Med*, vol. **25**, no. 2, pp. 423–433, Feb. 2014.
[27] I. Bružauskaitė, D. Bironaitė, E. Bagdonas, and E. Bernotienė, "Scaffolds and cells for tissue regeneration: different scaffold pore sizes—different cell effects," *Cytotechnology 2015 68:3*, vol. **68**, no. 3, pp. 355–369, Jun. 2015.
[28] I. Ćorković, A. Pichler, J. Šimunović, and M. Kopjar, "Hydrogels: Characteristics and Application as Delivery Systems of Phenolic and Aroma Compounds," *Foods*, vol. **10**, no. 6, Jun. 2021.
[29] C. D. Bucak and M. O. Sahin, "Super-flexible, moldable, injectable, self-healing PVA/B/CMC hydrogels synthesis and characterization, as potential water-retaining agent in agriculture," *Polymer Bulletin*, vol. **80**, no. 6, pp. 6591–6608, Jun. 2023.
[30] A. A. P. Mansur, M. A. Rodrigues, N. S. V. Capanema, S. M. Carvalho, D. A. Gomes, and H. S. Mansur, "Functionalized bioadhesion-enhanced carboxymethyl cellulose/polyvinyl alcohol hybrid hydrogels for chronic wound dressing applications," *RSC Adv*, vol. **13**, no. 19, pp. 13156–13168, Apr. 2023.
[31] A. Sood, M. S. Granick, and N. L. Tomaselli, "Wound Dressings and Comparative Effectiveness Data," *Adv Wound Care (New Rochelle)*, vol. **3**, no. 8, p. 511, Aug. 2014.
[32] Ajazuddin *et al.*, "Recent expansions in an emergent novel drug delivery technology: Emulgel," *Journal of Controlled Release*, vol. **171**, no. 2, pp. 122–132, Oct. 2013.
[33] P. Liu, M. Zhai, J. Li, J. Peng, and J. Wu, "Radiation preparation and swelling behavior of sodium carboxymethyl cellulose hydrogels," 2002.
[34] N. P. Esfahani, N. Koupaei, and H. Bahreini, "Fabrication and characterization of a novel hydrogel network composed of polyvinyl alcohol/polyvinylpyrrolidone/nano-rGO as wound dressing application," *Journal of Polymer Research*, vol. **30**, no. 2, pp. 1–15, Feb. 2023.
[35] C. Greene, H. T. Beaman, D. Stinfort, M. Ramezani, and M. B. B. Monroe, "Antimicrobial PVA Hydrogels with Tunable Mechanical Properties and Antimicrobial Release Profiles," *Journal of Functional Biomaterials* 2023, Vol. **14**, Page 234, Apr. 2023.